

Jeffrey A. Fessler

EECS Department, BME Department, Dept. of Radiology
University of Michigan

<http://web.eecs.umich.edu/~fessler>

ISMRM Data Sampling & Image Reconstruction Workshop
Sedona, AZ
2026-01-12

Declaration: No relevant financial interests or relationships to disclose

Declaration of Relevant Financial Interests or Relationships

Speaker Name: Jeff Fessler

I have no conflicts of interest with regards to MR topics.

Introduction

Adjoint

Preconditioning

Regularization/Priors

Convexity

Proximal operators

Low-rank models

Summary

Bibliography

(with ML connections...)

- ▶ Spin preparation RF pulse(s)
 $m(\vec{r}, 0)$ magnetization encoding relaxation, diffusion, velocity, ...
- ▶ Bloch equation (or Bloch-McConnell or Bloch-Torrey)
for transverse magnetization free precession after i th pulse

$$m(\vec{r}, t) = m(\vec{r}, 0) e^{-R_2(\vec{r})t} e^{-i\phi_i(\vec{r}, t)}$$

phase ϕ depends on gradient fields, off-resonance, ...

- ▶ Signal model for i th readout:

$$s_i(t) = \int m(\vec{r}, t) d\vec{r} = \int m(\vec{r}, 0) e^{-R_2(\vec{r})t} e^{-i\phi_i(\vec{r}, t)} d\vec{r}$$

- ▶ Discretization of integral:

$$\mathbf{s} \approx \mathbf{A}\mathbf{x}, \quad x_j \triangleq m(\vec{r}_j, 0)$$

\mathbf{A} depends on physics: gradients, coil maps, ...

- ▶ Noisy measurements (thermal noise): $\mathbf{y} = \mathbf{s} + \boldsymbol{\varepsilon} = \mathbf{A}\mathbf{x} + \boldsymbol{\varepsilon}$
- ▶ probability model: $\boldsymbol{\varepsilon} \sim \mathcal{CN}(\mathbf{0}, \sigma^2 \mathbf{I})$

$$p(\mathbf{y} | \mathbf{x}) \propto \exp\left(-\frac{1}{2\sigma^2} \|\mathbf{y} - \mathbf{A}\mathbf{x}\|_2^2\right)$$

(after pre-whitening of correlation between multiple receive coils)

- ▶ negative log-likelihood:

$$-\log p(\mathbf{y} | \mathbf{x}) = \frac{1}{2\sigma^2} \|\mathbf{A}\mathbf{x} - \mathbf{y}\|_2^2$$

apt for any k-space sampling pattern, including non-Cartesian and non-Fourier encoding

- ▶ **Gauss-Markov theorem** provides some theoretical basis for this data-fit term
- ▶

- ▶ Noisy measurements (thermal noise): $\mathbf{y} = \mathbf{s} + \boldsymbol{\varepsilon} = \mathbf{A}\mathbf{x} + \boldsymbol{\varepsilon}$
- ▶ probability model: $\boldsymbol{\varepsilon} \sim \mathcal{CN}(\mathbf{0}, \sigma^2 \mathbf{I})$

$$p(\mathbf{y} | \mathbf{x}) \propto \exp\left(-\frac{1}{2\sigma^2} \|\mathbf{y} - \mathbf{A}\mathbf{x}\|_2^2\right)$$

(after pre-whitening of correlation between multiple receive coils)

- ▶ negative log-likelihood:

$$-\log p(\mathbf{y} | \mathbf{x}) = \frac{1}{2\sigma^2} \|\mathbf{A}\mathbf{x} - \mathbf{y}\|_2^2$$

apt for any k-space sampling pattern, including non-Cartesian and non-Fourier encoding

- ▶ **Gauss-Markov theorem** provides some theoretical basis for this data-fit term
- ▶ Other important statistical models in MRI
 - ▶ physiological “noise” in fMRI
 - ▶ particle diffusion distributions
 - ▶ ...

- ▶ Goal of (basic) image reconstruction is to recover magnetization image \mathbf{x} from k-space data \mathbf{y} using negative log-likelihood:

$$f(\mathbf{x}) = -\log p(\mathbf{y} | \mathbf{x}) = \frac{1}{2} \|\mathbf{Ax} - \mathbf{y}\|_2^2$$

(Drop constant σ^2 : unimportant for regularized methods, but more important for Bayesian methods.)

- ▶ Iterative methods are used when \mathbf{A} is non-square (and hence non-invertible)
- ▶ Most iterative methods use the *gradient* of the data-fit term:

$$\nabla f(\mathbf{x}) = \mathbf{A}'(\mathbf{Ax} - \mathbf{y})$$

where \mathbf{A}' denotes the *adjoint* of matrix/operator \mathbf{A}



- ▶ Goal of (basic) image reconstruction is to recover magnetization image \mathbf{x} from k-space data \mathbf{y} using negative log-likelihood:

$$f(\mathbf{x}) = -\log p(\mathbf{y} | \mathbf{x}) = \frac{1}{2} \|\mathbf{Ax} - \mathbf{y}\|_2^2$$

(Drop constant σ^2 : unimportant for regularized methods, but more important for Bayesian methods.)

- ▶ Iterative methods are used when \mathbf{A} is non-square (and hence non-invertible)
- ▶ Most iterative methods use the *gradient* of the data-fit term:

$$\nabla f(\mathbf{x}) = \mathbf{A}'(\mathbf{Ax} - \mathbf{y})$$

where \mathbf{A}' denotes the *adjoint* of matrix/operator \mathbf{A}

- ▶ The “ \mathbf{A} ” written on paper is rarely a (dense) matrix in MRI recon software.

Adjoints

- ▶ Dynamic MRI data-fit term:

$$f(\mathbf{X}) = \frac{1}{2} \|\mathcal{A}\mathbf{X} - \mathbf{y}\|_2^2$$

- Casorati matrix $\mathbf{X} = [\mathbf{x}_1 \ \dots \ \mathbf{x}_T] \in \mathbb{C}^{N \times T}$ (# of voxels \times # of time frames)
- Linear operator \mathcal{A} maps array \mathbf{X} into k-space signal data vector $\mathbf{s} \in \mathbb{C}^M$:

$$\mathcal{A}\mathbf{X} = \begin{bmatrix} \mathbf{A}_1 \mathbf{x}_1 \\ \vdots \\ \mathbf{A}_T \mathbf{x}_T \end{bmatrix} \quad (\mathbf{A}_t \text{ is encoding for } t\text{th frame})$$



- ▶ Dynamic MRI data-fit term:

$$f(\mathbf{X}) = \frac{1}{2} \|\mathcal{A}\mathbf{X} - \mathbf{y}\|_2^2$$

- Casorati matrix $\mathbf{X} = [\mathbf{x}_1 \ \dots \ \mathbf{x}_T] \in \mathbb{C}^{N \times T}$ (# of voxels \times # of time frames)
- Linear operator \mathcal{A} maps array \mathbf{X} into k-space signal data vector $\mathbf{s} \in \mathbb{C}^M$:

$$\mathcal{A}\mathbf{X} = \begin{bmatrix} \mathbf{A}_1 \mathbf{x}_1 \\ \vdots \\ \mathbf{A}_T \mathbf{x}_T \end{bmatrix} \quad (\mathbf{A}_t \text{ is encoding for } t\text{th frame})$$

- ▶ Gradient of dynamic MRI data-fit term:

$$\nabla f(\mathbf{X}) = \mathcal{A}'(\mathcal{A}\mathbf{X} - \mathbf{y})$$

- ▶ \mathcal{A} is not a matrix, but it has a well-defined adjoint needed for the gradient:

$$\mathcal{A}'\mathbf{y} = [\mathbf{A}'_1 \mathbf{y}_1 \ \dots \ \mathbf{A}'_T \mathbf{y}_T] \quad (\text{maps vector to matrix})$$

- ▶ Linear operator $\mathcal{A} : \mathcal{X} \mapsto \mathcal{Y}$
 \mathcal{X} vector space with inner product $\langle \cdot, \cdot \rangle_{\mathcal{X}}$
 \mathcal{Y} vector space with inner product $\langle \cdot, \cdot \rangle_{\mathcal{Y}}$
- ▶ The **(Hermitian) adjoint** of \mathcal{A} is the *unique* operator \mathcal{A}' satisfying

$$\langle \mathcal{A}\mathbf{x}, \mathbf{y} \rangle_{\mathcal{Y}} = \langle \mathbf{x}, \mathcal{A}'\mathbf{y} \rangle_{\mathcal{X}}, \quad \forall \mathbf{x} \in \mathcal{X}, \mathbf{y} \in \mathcal{Y}$$



- ▶ Linear operator $\mathcal{A} : \mathcal{X} \mapsto \mathcal{Y}$
 \mathcal{X} vector space with inner product $\langle \cdot, \cdot \rangle_{\mathcal{X}}$
 \mathcal{Y} vector space with inner product $\langle \cdot, \cdot \rangle_{\mathcal{Y}}$
- ▶ The **(Hermitian) adjoint** of \mathcal{A} is the *unique* operator \mathcal{A}' satisfying

$$\langle \mathcal{A}\mathbf{x}, \mathbf{y} \rangle_{\mathcal{Y}} = \langle \mathbf{x}, \mathcal{A}'\mathbf{y} \rangle_{\mathcal{X}}, \quad \forall \mathbf{x} \in \mathcal{X}, \mathbf{y} \in \mathcal{Y}$$

- ▶ An adjoint usually is not inverse nor pseudoinverse: $\mathcal{A}' \neq \mathcal{A}^{-1}$ and $\mathcal{A}' \neq \mathcal{A}^+$
- ▶ Notable exception: single-coil MRI, full Cartesian k-space sampling, unitary FFT
- ▶

- ▶ Linear operator $\mathcal{A} : \mathcal{X} \mapsto \mathcal{Y}$
 \mathcal{X} vector space with inner product $\langle \cdot, \cdot \rangle_{\mathcal{X}}$
 \mathcal{Y} vector space with inner product $\langle \cdot, \cdot \rangle_{\mathcal{Y}}$
- ▶ The **(Hermitian) adjoint** of \mathcal{A} is the *unique* operator \mathcal{A}' satisfying

$$\langle \mathcal{A}\mathbf{x}, \mathbf{y} \rangle_{\mathcal{Y}} = \langle \mathbf{x}, \mathcal{A}'\mathbf{y} \rangle_{\mathcal{X}}, \quad \forall \mathbf{x} \in \mathcal{X}, \mathbf{y} \in \mathcal{Y}$$

- ▶ An adjoint usually is not inverse nor pseudoinverse: $\mathcal{A}' \neq \mathcal{A}^{-1}$ and $\mathcal{A}' \neq \mathcal{A}^+$
- ▶ Notable exception: single-coil MRI, full Cartesian k-space sampling, unitary FFT
- ▶ Be wary of code that provides untested “adjoint” functions:
 - “Adjoint” code with density compensation
 - “Adjoint” code for `fft` based on `ifft`
 FFTW library provides `bfft` for adjoint of `fft`

Testing adjoints of complicated linear operators

- ▶ Random vector test (large scale) using definition:

$$\langle \mathcal{A}\mathbf{x}, \mathbf{y} \rangle_{\mathcal{Y}} \approx \langle \mathbf{x}, \mathcal{A}'\mathbf{y} \rangle_{\mathcal{X}}, \quad \text{for random } \mathbf{x} \in \mathcal{X} \text{ and } \mathbf{y} \in \mathcal{Y}$$

- ▶ Exhaustive test (small scale):

$$\langle \mathcal{A}\mathbf{e}_j, \mathbf{e}_i \rangle_{\mathcal{Y}} \approx \langle \mathbf{e}_j, \mathcal{A}'\mathbf{e}_i \rangle_{\mathcal{X}}, \quad \forall i, j$$

| Recon Package | Random Tests | Exhaustive Tests |
|-----------------------|--------------|------------------|
| BART (C) | Y | |
| MatMRI (Matlab) | Y | |
| MIRTorCh (pytorch) | Y | |
| MIRT.jl (Julia) | Y | Y |
| MIRT classic (Matlab) | Y | Y |
| PySap-MRI | Y | |
| SigPy | Y | |

- ▶ Another option: let `autodiff` do the work [1]
- ▶ “FAST-DIPS: Adjoint-free analytic steps and hard-constrained likelihood correction for diffusion-prior inverse problems”

ICLR 2026 Submission <https://openreview.net/forum?id=voMeZVAkKL>

Preconditioning

- ▶ A **preconditioner** helps find the *same solution* but *faster*.
- ▶ Solving system of equations
 - $\mathbf{Ax} = \mathbf{b}$
 - \mathbf{A} is square and invertible
 - Left preconditioner: $\mathbf{PAx} = \mathbf{Pb}$. Same solution if \mathbf{P} is invertible.
- ▶

- ▶ A **preconditioner** helps find the *same solution* but *faster*.
- ▶ Solving system of equations
 - $\mathbf{Ax} = \mathbf{b}$
 - \mathbf{A} is square and invertible
 - Left preconditioner: $\mathbf{PAx} = \mathbf{Pb}$. Same solution if \mathbf{P} is invertible.
- ▶ In iterative MRI reconstruction, \mathbf{A} is rarely square or invertible!
- ▶ Solving an optimization problem based on log-likelihood
$$\hat{\mathbf{x}} = \arg \min_{\mathbf{x}} \Psi(\mathbf{x}), \quad \Psi(\mathbf{x}) \triangleq \frac{1}{2} \|\mathbf{Ax} - \mathbf{y}\|_2^2 + \beta R(\mathbf{x})$$
- ▶

- ▶ A **preconditioner** helps find the *same solution* but *faster*.
- ▶ Solving system of equations
 - $\mathbf{Ax} = \mathbf{b}$
 - \mathbf{A} is square and invertible
 - Left preconditioner: $\mathbf{PAx} = \mathbf{Pb}$. Same solution if \mathbf{P} is invertible.
- ▶ In iterative MRI reconstruction, \mathbf{A} is rarely square or invertible!
- ▶ Solving an optimization problem based on log-likelihood
$$\hat{\mathbf{x}} = \arg \min_{\mathbf{x}} \Psi(\mathbf{x}), \quad \Psi(\mathbf{x}) \triangleq \frac{1}{2} \|\mathbf{Ax} - \mathbf{y}\|_2^2 + \beta R(\mathbf{x})$$
- ▶ Left-multiplying \mathbf{A} *changes* the solution [2, 3] and increases noise [4]:
$$\mathbf{x}_? = \arg \min_{\mathbf{x}} \frac{1}{2} \|\mathbf{WAx} - \mathbf{Wy}\|_2^2 + \beta R(\mathbf{x})$$
 (“weighting” not “preconditioning”)
- ▶

- ▶ A **preconditioner** helps find the *same solution* but *faster*.
- ▶ Solving system of equations
 - $\mathbf{Ax} = \mathbf{b}$
 - \mathbf{A} is square and invertible
 - Left preconditioner: $\mathbf{PAx} = \mathbf{Pb}$. Same solution if \mathbf{P} is invertible.
- ▶ In iterative MRI reconstruction, \mathbf{A} is rarely square or invertible!
- ▶ Solving an optimization problem based on log-likelihood

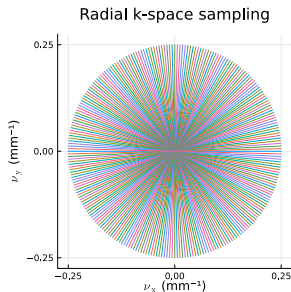
$$\hat{\mathbf{x}} = \arg \min_{\mathbf{x}} \Psi(\mathbf{x}), \quad \Psi(\mathbf{x}) \triangleq \frac{1}{2} \|\mathbf{Ax} - \mathbf{y}\|_2^2 + \beta R(\mathbf{x})$$
- ▶ Left-multiplying \mathbf{A} *changes* the solution [2, 3] and increases noise [4]:

$$\mathbf{x}_? = \arg \min_{\mathbf{x}} \frac{1}{2} \|\mathbf{WAx} - \mathbf{Wy}\|_2^2 + \beta R(\mathbf{x}) \quad (\text{"weighting" not "preconditioning"})$$
- ▶ One should precondition in a way that *preserves* the solution [5], e.g.:

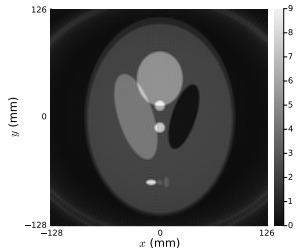
$$\mathbf{x}_{k+1} = \mathbf{x}_k - \mathbf{P}\nabla\Psi(\mathbf{x}_k). \quad \text{Ideally } \mathbf{P} \approx (\nabla^2\Psi)^{-1} \quad (\text{not any DCF})$$

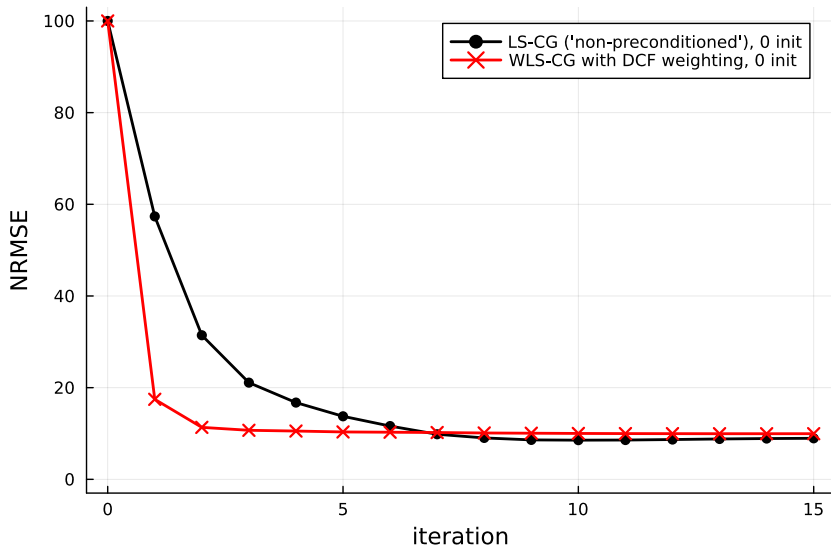
<https://juliaimagerecon.github.io/Examples/generated/mri/6-precon>

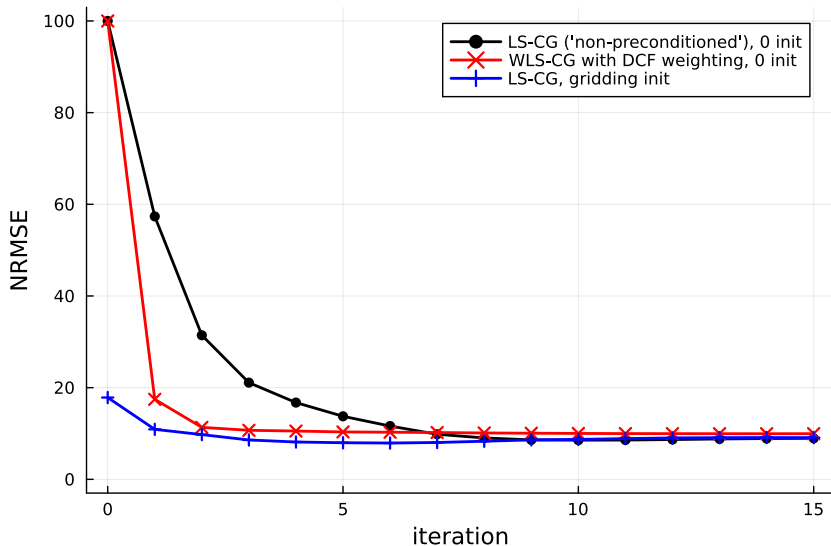
- ▶ analytical k-space from ellipse Fourier transform (no inverse crime) [6, 7]
- ▶ 128×128 image reconstruction
- ▶ 126 radial lines with 129 samples each
- ▶ Examine $\text{NRMSE} = 100\% \cdot \|\hat{\mathbf{x}}_k - \mathbf{x}_{\text{true}}\|_2 / \|\mathbf{x}_{\text{true}}\|_2$ vs iteration $k = 0, 1, \dots$



NUFFT gridding with better ramp-filter DCF









- ▶ Pruessmann et al., MRM 2001 [2]
- ▶ Gabr et al., MRM 2006 [4]
- ▶ Baron et al., MRM 2018 [3]
- ▶ Ong et al., IEEE T-MI 2020 [5]
- ▶

- ▶ Pruessmann et al., MRM 2001 [2]
- ▶ Gabr et al., MRM 2006 [4]
- ▶ Baron et al., MRM 2018 [3]
- ▶ Ong et al., IEEE T-MI 2020 [5]
- ▶ Hong et al., IEEE T-CI 2024 [8]

1476

IEEE TRANSACTIONS ON COMPUTATIONAL IMAGING, VOL. 10, 2024

Provable Preconditioned Plug-and-Play Approach for Compressed Sensing MRI Reconstruction

Tao Hong[✉], Member, IEEE, Xiaojian Xu[✉], Member, IEEE, Jason Hu[✉], Graduate Student Member, IEEE,
and Jeffrey A. Fessler[✉], Fellow, IEEE

$$\mathbf{x}_{k+1} = \arg \min_{\mathbf{x}} \frac{1}{2} \|\mathbf{x} - (\mathbf{x}_k - \alpha \mathbf{P} \nabla f(\mathbf{x}_k))\|_2^2 + \frac{\beta}{\|\mathbf{P}^{-1}\|_2} R(\mathbf{x}).$$

- ▶ Hong et al., IEEE T-CI 2025 [9]

1630

IEEE TRANSACTIONS ON COMPUTATIONAL IMAGING, VOL. 11, 2025

Using Randomized Nyström Preconditioners to Accelerate Variational Image Reconstruction

Tao Hong[✉], Member, IEEE, Zhaoyi Xu[✉], Jason Hu[✉], Graduate Student Member, IEEE,
and Jeffrey A. Fessler[✉], Fellow, IEEE

- ▶ 2025-12-05 arXiv submission: (MRM submit) [10]

Fast and Robust Diffusion Posterior Sampling for
MR Image Reconstruction Using the
Preconditioned Unadjusted Langevin Algorithm

Moritz Blumenthal^{*1}, Tina Holliber^{*1}, Jonathan I. Tamir^{2,3}, and
Martin Uecker^{1,4}



- ▶ 2025-12-05 arXiv submission: (MRM submit) [10]

Fast and Robust Diffusion Posterior Sampling for
MR Image Reconstruction Using the
Preconditioned Unadjusted Langevin Algorithm

Moritz Blumenthal^{*1}, Tina Holliber^{*1}, Jonathan I. Tamir^{2,3}, and
Martin Uecker^{1,4}



$$\mathbf{x}_t^{k+1} = \mathbf{x}_t^k + \gamma M_t \left[A^H (\mathbf{y} - A \mathbf{x}_t^k) + \nabla_{\bar{\mathbf{x}}} \log p_t(\mathbf{x}_t^k) \right] + \sqrt{2\gamma} \mathbf{z}^k \quad \mathbf{z}^k \sim \mathbb{CN}(\mathbf{0}, M_t^{-1})$$

(8)

Regularization/Priors

- ▶ Priors or regularizers are essential for under-sampled data

$$\hat{\mathbf{x}}_{\text{MAP}} = \arg \max_{\mathbf{x}} p(\mathbf{x} | \mathbf{y}) = \arg \max_{\mathbf{x}} \log p(\mathbf{y} | \mathbf{x}) + \log p(\mathbf{x})$$

$$\hat{\mathbf{x}}_{\text{RegLS}} = \arg \min_{\mathbf{x}} \frac{1}{2} \|\mathbf{Ax} - \mathbf{y}\|_2^2 + \beta R(\mathbf{x})$$

$$p(\mathbf{x}) \propto e^{-\beta R(\mathbf{x})}$$

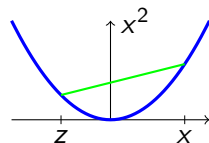
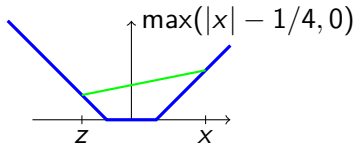
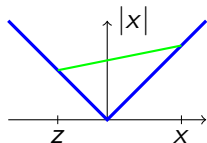
- ▶ Modeling choices: $p(\mathbf{x})$ and/or $\beta R(\mathbf{x})$
- ▶ Iterative optimization algorithms: choices/challenges

Convexity

- ▶ Convex function definition:

$$f(\alpha \mathbf{x} + (1 - \alpha)\mathbf{z}) \leq \alpha f(\mathbf{x}) + (1 - \alpha)f(\mathbf{z}), \quad \forall \mathbf{x}, \mathbf{z}, \quad \forall 0 \leq \alpha \leq 1$$

- ▶ 1D examples:



- ▶ All local minimizers are global minimizers.
- ▶ Popular convex regularizers in MRI:

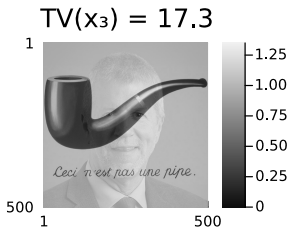
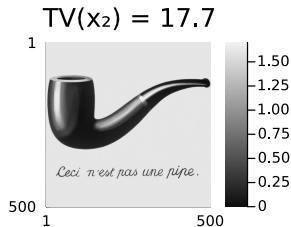
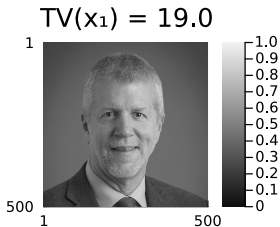
- ▶ Total variation (TV); in 1D: $R(\mathbf{x}) = \sum_n |x_n - x_{n-1}| = \|\mathbf{D}\mathbf{x}\|_1$,

$$\mathbf{D} = \begin{bmatrix} -1 & 1 & 0 & \dots \\ & \ddots & \ddots & \\ \dots & 0 & -1 & 1 \end{bmatrix}$$

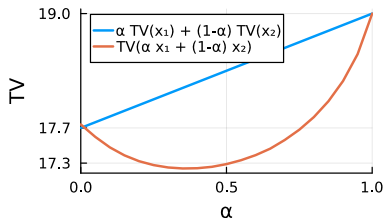
- ▶ 1-norm of wavelet transform: $R(\mathbf{x}) = \|\mathbf{W}\mathbf{x}\|_1$, $\|\mathbf{v}\|_1 = \sum_i |v_i|$

<https://radiology.wisc.edu/profile/james-pipe-2758>

The Treachery of Images: René Magritte, 1929

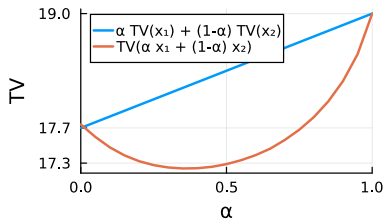
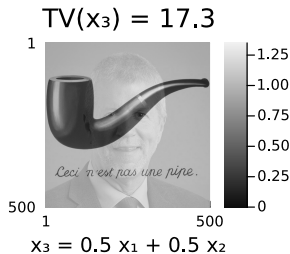
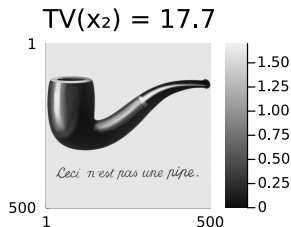
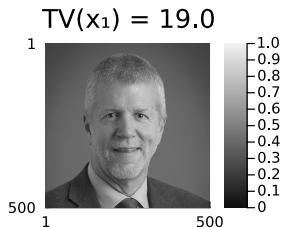


$$x_3 = 0.5 x_1 + 0.5 x_2$$



<https://radiology.wisc.edu/profile/james-pipe-2758>

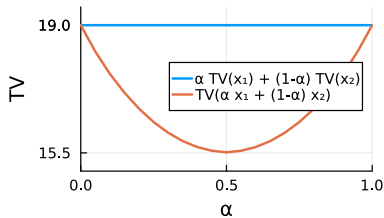
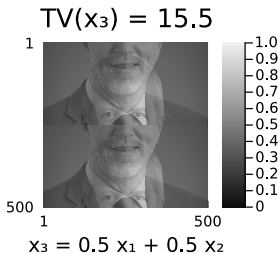
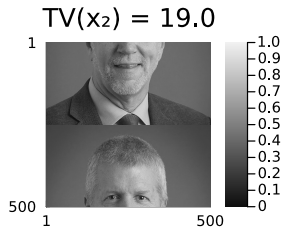
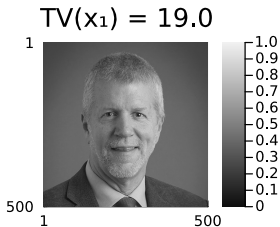
The Treachery of Images: René Magritte, 1929



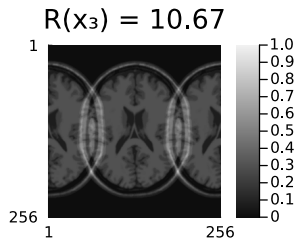
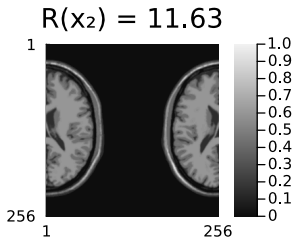
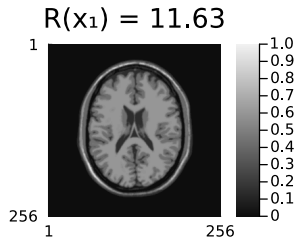
- ▶ TV vs “sparsity”?
- ▶ Inherent to convex regularizers
- ▶ Bayesian view: $p(\mathbf{x}) \propto e^{-\beta R(\mathbf{x})}$

<https://radiology.wisc.edu/profile/james-pipe-2758>

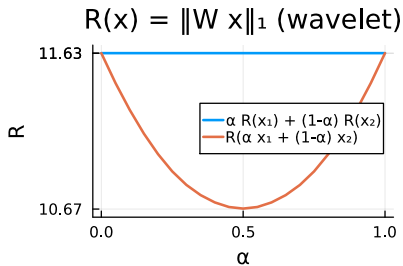
The Treachery of Images: René Magritte, 1929



- ▶ TV vs “sparsity”?
- ▶ Inherent to convex regularizers
- ▶ Bayesian view:
 $p(\mathbf{x}) \propto e^{-\beta R(\mathbf{x})}$

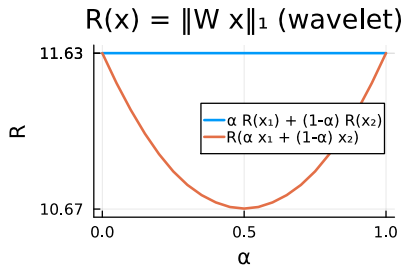
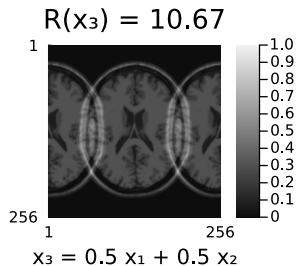
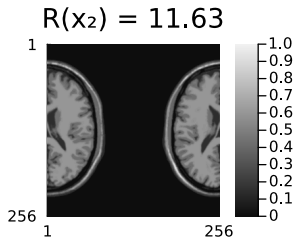
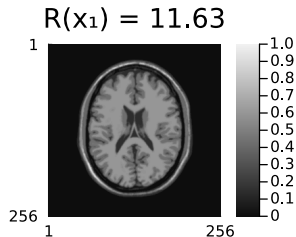


$$x_3 = 0.5 x_1 + 0.5 x_2$$



▶ BrainWeb
phantom [11]

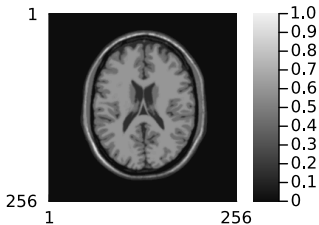




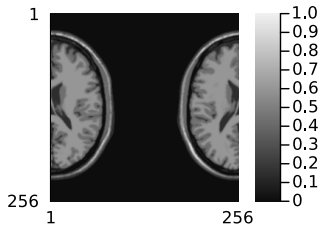
► BrainWeb
phantom [11]

► Similar plots in Lobos
et al. IEEE T-MI 2018
[12] for structured
low-rank regularizer

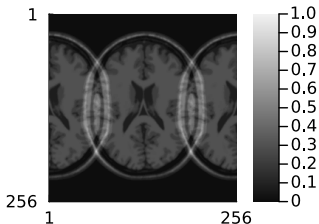
$R(x_1) = 90.01$



$R(x_2) = 90.01$



$R(x_3) = 109.17$

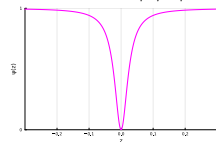


$x_3 = 0.5 x_1 + 0.5 x_2$

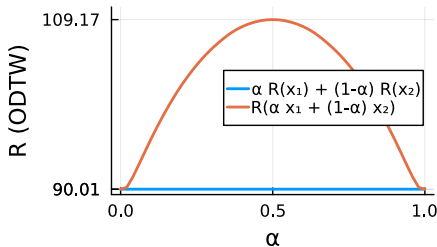
Geman/McClure

potential [13]:

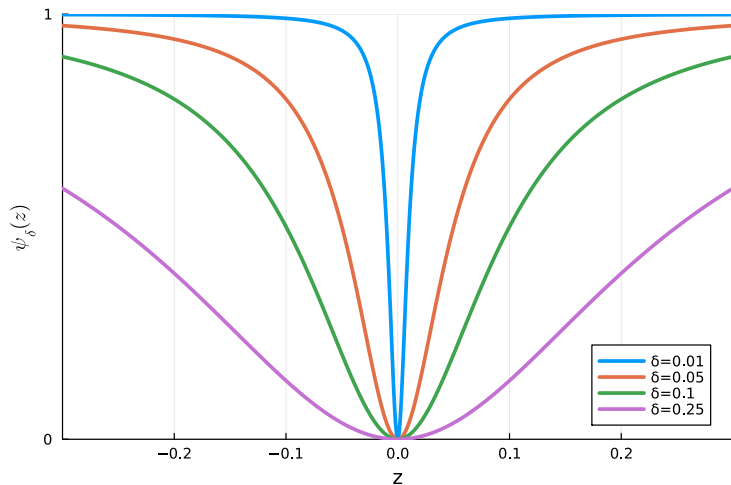
$$\psi(z) = \frac{|z/\delta|^2}{1+|z/\delta|^2}$$



$R(x)$: Geman/McClure



$$R(x) = \sum_i \psi([Wx]_i) \approx \|Wx\|_0$$



- One convex run to get a decent initial \mathbf{x}_0
followed by non-convex optimization to get $\hat{\mathbf{x}}$ often works fine [14]

- ▶ Convex regularizers cannot really measure “sparsity”
- ▶ Most neural network “regularizers” are non-convex
- ▶ Some notable exceptions:
 - Goujon et al., SIAM IS 2024 [15]
 - Chand & Jacob, ISMRM 2025 #5153 [16]
- ▶ Comparing a fancy deep network to TV/Wavelet with 1-norm is unfair?

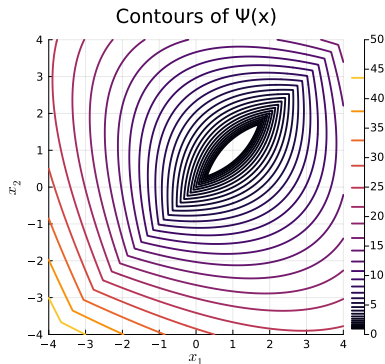
Proximal operators

- ▶ Classical compressed sensing uses 1-norm regularizers:

$$\hat{\mathbf{x}} = \arg \min_{\mathbf{x} \in \mathbb{C}^N} \Psi(\mathbf{x}), \quad \Psi(\mathbf{x}) \triangleq \frac{1}{2} \|\mathbf{Ax} - \mathbf{y}\|_2^2 + \beta \|\mathbf{T}\mathbf{x}\|_1$$

for some choices of matrix \mathbf{T} (e.g., finite differences or wavelets...)

- ▶ The 1-norm causes non-differentiable Ψ :



- ▶ Classical compressed sensing uses 1-norm regularizers:

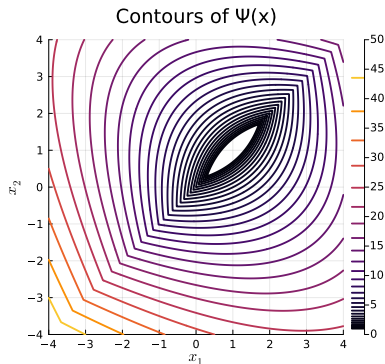
$$\hat{\mathbf{x}} = \arg \min_{\mathbf{x} \in \mathbb{C}^N} \Psi(\mathbf{x}), \quad \Psi(\mathbf{x}) \triangleq \frac{1}{2} \|\mathbf{Ax} - \mathbf{y}\|_2^2 + \beta \|\mathbf{T}\mathbf{x}\|_1$$

for some choices of matrix \mathbf{T} (e.g., finite differences or wavelets...)

- ▶ The 1-norm causes non-differentiable Ψ :

- ▶ Options:

- Use subgradient methods
 - slow convergence
- Round corner of absolute value
 - ▶ make Ψ differentiable
 - ▶ lose “sparsity” but...
- Use proximal methods
 - ▶ convergence guarantees
 - ▶ closely related to many ML methods



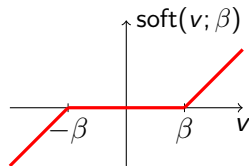
Given a function $f : \mathcal{X} \mapsto \mathbb{R}$ the **proximal operator** is

$$\text{prox}_f(\mathbf{v}) \triangleq \arg \min_{\mathbf{x} \in \mathcal{X}} \left\{ \frac{1}{2} \|\mathbf{x} - \mathbf{v}\|_{\mathcal{X}}^2 + f(\mathbf{x}) \right\}.$$

cf Fourier transform

Important and easy case:

$$f(\mathbf{x}) = \beta \|\mathbf{x}\|_1 \implies \text{prox}_f(\mathbf{v}) = \text{soft}(\mathbf{v}, \beta)$$



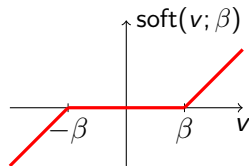
Given a function $f : \mathcal{X} \mapsto \mathbb{R}$ the **proximal operator** is

$$\text{prox}_f(\mathbf{v}) \triangleq \arg \min_{\mathbf{x} \in \mathcal{X}} \left\{ \frac{1}{2} \|\mathbf{x} - \mathbf{v}\|_{\mathcal{X}}^2 + f(\mathbf{x}) \right\}.$$

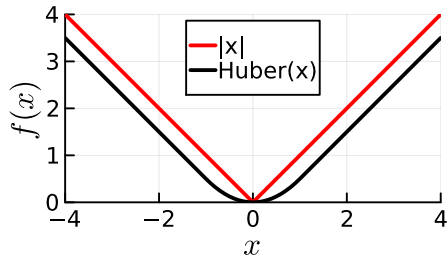
cf Fourier transform

Important and easy case:

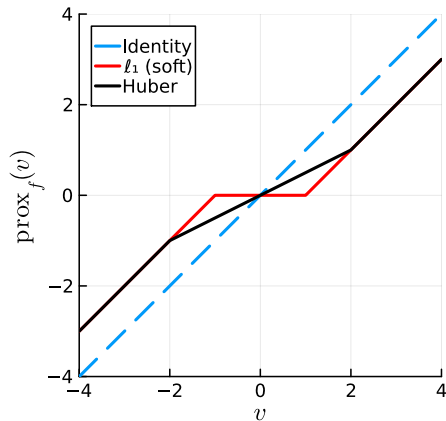
$$f(\mathbf{x}) = \beta \|\mathbf{x}\|_1 \implies \text{prox}_f(\mathbf{v}) = \text{soft}(\mathbf{v}, \beta)$$



- ▶ flat region \implies sparsity
- ▶ closely related to ReLU in NN models



Corner rounding \implies less sparsity





- ▶ Easy case: for a **unitary matrix** \mathbf{W} (e.g., orthogonal wavelet transform):

$$f(\mathbf{x}) = \beta \|\mathbf{W}\mathbf{x}\|_1 \implies \text{prox}_f(\mathbf{v}) = \mathbf{W}' \text{soft} .(\mathbf{W}\mathbf{v}, \beta)$$



- ▶ Easy case: for a **unitary matrix** \mathbf{W} (e.g., orthogonal wavelet transform):

$$f(\mathbf{x}) = \beta \|\mathbf{W}\mathbf{x}\|_1 \implies \text{prox}_f(\mathbf{v}) = \mathbf{W}' \text{soft}(\mathbf{W}\mathbf{v}, \beta)$$

- ▶ The finite-difference matrix (cf. TV) $\mathbf{D} = \begin{bmatrix} -1 & 1 & 0 & \dots \\ & \ddots & & \\ \dots & 0 & -1 & 1 \end{bmatrix}$ is *not* unitary, so

$$f(\mathbf{x}) = \beta \|\mathbf{D}\mathbf{x}\|_1 \not\Rightarrow \text{prox}_f(\mathbf{v}) = \mathbf{D}' \text{soft}(\mathbf{D}\mathbf{x}, \beta).$$

(not hypothetical...)

- ▶ Iterative algorithms (e.g., ADMM, dual methods) are needed for TV proximal mapping [17, 18].

- ▶ Regularized image reconstruction problem

$$\hat{\mathbf{x}} = \arg \min_{\mathbf{x}} \left(\frac{1}{2} \|\mathbf{Ax} - \mathbf{y}\|_2^2 + \beta R(\mathbf{x}) \right)$$

- ▶ For prox-friendly regularizers, use (convergent!) proximal gradient method (PGM):

$$\mathbf{x}_{k+1} = \text{prox}_{\beta R}(\mathbf{x}_k - \alpha \mathbf{A}'(\mathbf{Ax}_k - \mathbf{y}))$$

- ▶ $R(\mathbf{x}) = \beta \|\mathbf{Wx}\|_1$ leads to Iterative Shrinkage-Thresholding Algorithm (ISTA) [19]:

$$\mathbf{x}_{k+1} = \mathcal{D}_{\beta}(\mathbf{x}_k - \alpha \mathbf{A}'(\mathbf{Ax}_k - \mathbf{y})), \quad \mathcal{D}_{\beta}(\mathbf{x}) = \text{prox}_{\beta \|\mathbf{Wx}\|_1}(\mathbf{x}) = \mathbf{W}' \text{soft} .(\mathbf{Wx}, \beta)$$

(Use FISTA [20] or OPTISTA [21] or POGM [22] with restart [23] instead, not ADMM! [24, 25])



- ▶ Regularized image reconstruction problem

$$\hat{\mathbf{x}} = \arg \min_{\mathbf{x}} \left(\frac{1}{2} \|\mathbf{Ax} - \mathbf{y}\|_2^2 + \beta R(\mathbf{x}) \right)$$

- ▶ For prox-friendly regularizers, use (convergent!) proximal gradient method (PGM):

$$\mathbf{x}_{k+1} = \text{prox}_{\beta R}(\mathbf{x}_k - \alpha \mathbf{A}'(\mathbf{Ax}_k - \mathbf{y}))$$

- ▶ $R(\mathbf{x}) = \beta \|\mathbf{Wx}\|_1$ leads to Iterative Shrinkage-Thresholding Algorithm (ISTA) [19]:

$$\mathbf{x}_{k+1} = \mathcal{D}_{\beta}(\mathbf{x}_k - \alpha \mathbf{A}'(\mathbf{Ax}_k - \mathbf{y})), \quad \mathcal{D}_{\beta}(\mathbf{x}) = \text{prox}_{\beta \|\mathbf{Wx}\|_1}(\mathbf{x}) = \mathbf{W}' \text{soft} .(\mathbf{Wx}, \beta)$$

(Use FISTA [20] or OPTISTA [21] or POGM [22] with restart [23] instead, not ADMM! [24, 25])

- ▶ Denoising operation *cf.* plug-and-play methods, unrolled deep networks, etc.
Replace \mathcal{D}_{β} with ML denoiser (PNP survey [26])



- ▶ Regularized image reconstruction problem

$$\hat{\mathbf{x}} = \arg \min_{\mathbf{x}} \left(\frac{1}{2} \|\mathbf{Ax} - \mathbf{y}\|_2^2 + \beta R(\mathbf{x}) \right)$$

- ▶ For prox-friendly regularizers, use (convergent!) proximal gradient method (PGM):

$$\mathbf{x}_{k+1} = \text{prox}_{\beta R}(\mathbf{x}_k - \alpha \mathbf{A}'(\mathbf{Ax}_k - \mathbf{y}))$$

- ▶ $R(\mathbf{x}) = \beta \|\mathbf{Wx}\|_1$ leads to Iterative Shrinkage-Thresholding Algorithm (ISTA) [19]:

$$\mathbf{x}_{k+1} = \mathcal{D}_{\beta}(\mathbf{x}_k - \alpha \mathbf{A}'(\mathbf{Ax}_k - \mathbf{y})), \quad \mathcal{D}_{\beta}(\mathbf{x}) = \text{prox}_{\beta \|\mathbf{Wx}\|_1}(\mathbf{x}) = \mathbf{W}' \text{soft} .(\mathbf{Wx}, \beta)$$

(Use FISTA [20] or OPTISTA [21] or POGM [22] with restart [23] instead, not ADMM! [24, 25])

- ▶ Denoising operation *cf.* plug-and-play methods, unrolled deep networks, etc.
Replace \mathcal{D}_{β} with ML denoiser (PNP survey [26])
- ▶ Convergence? [27–35]

Convergent Complex Quasi-Newton Proximal Methods for Gradient-Driven Denoisers in Compressed Sensing MRI Reconstruction

Tao Hong , *Member, IEEE*, Zhaoyi Xu , Se Young Chun , *Member, IEEE*, Luis Hernandez-Garcia ,
and Jeffrey A. Fessler , *Fellow, IEEE*

$$\mathbf{x}_{k+1} = \text{prox}_{\alpha_k f}^{B_k}(\mathbf{x}_k - \alpha_k P_k \nabla R_{\theta}(\mathbf{x}))$$



Convergent Complex Quasi-Newton Proximal Methods for Gradient-Driven Denoisers in Compressed Sensing MRI Reconstruction

Tao Hong , *Member, IEEE*, Zhaoyi Xu , Se Young Chun , *Member, IEEE*, Luis Hernandez-Garcia ,
and Jeffrey A. Fessler , *Fellow, IEEE*

$$\mathbf{x}_{k+1} = \text{prox}_{\alpha_k f}^{\mathbf{B}_k}(\mathbf{x}_k - \alpha_k \mathbf{P}_k \nabla R_\theta(\mathbf{x}))$$

- ▶ Preconditioning (iteration-dependent) \mathbf{B}_k , \mathbf{P}_k via quasi-Newton rank-1 updates
- ▶ Non-convex learned regularizer R_θ
- ▶ (Weighted) proximal operator (uses adjoint of \mathbf{A})
- ▶ Convergence

Low-rank models

Smooth optimization using global and local low-rank regularizers

Rodrigo A. Lobos^{†*}, Javier Salazar Cavazos[†], Raj Rao Nadakuditi[†], and Jeffrey A. Fessler[†]

- ▶ Differentiable tail singular value regularizer:

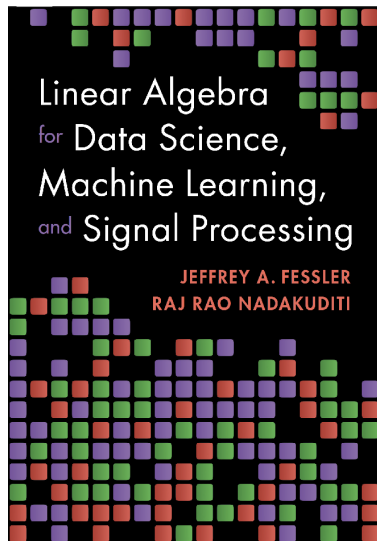
$$R(\mathbf{X}) = \sum_{k=K+1}^r \psi(\sigma_k(\mathbf{X}))$$

- ▶ Non-convex if $K > 0$ or if ψ is non-convex.
- ▶ Differentiable if ψ is.
- ▶ Nonlinear CG or quasi-Newton optimizers
- ▶ Reduced NRMSE LLR reconstructions for dynamic MRI
Lobos et al., SIAM IS 2026 [36, 37]

- ▶ Many opportunities to “abuse math” in iterative image reconstruction field
 - ▶ Mismatched adjoint operators
 - ▶ DCF-based weighting that does not match the log-likelihood
 - ▶ Incorrect proximal mappings
 - ▶ Replacing proximal operators with deep networks with unknown properties
 - ▶ ...
- ▶

- ▶ Many opportunities to “abuse math” in iterative image reconstruction field
 - ▶ Mismatched adjoint operators
 - ▶ DCF-based weighting that does not match the log-likelihood
 - ▶ Incorrect proximal mappings
 - ▶ Replacing proximal operators with deep networks with unknown properties
 - ▶ ...
- ▶ Other topics:
 - ▶ Early stopping of CG as a means of regularization
 - ▶ Hidden cost function modifications like corner rounding
 - ▶ Using NRMSE and SSIM instead of task-relevant metrics
 - ▶ Inverse crimes [6, 38]
- ▶

- ▶ Many opportunities to “abuse math” in iterative image reconstruction field
 - ▶ Mismatched adjoint operators
 - ▶ DCF-based weighting that does not match the log-likelihood
 - ▶ Incorrect proximal mappings
 - ▶ Replacing proximal operators with deep networks with unknown properties
 - ▶ ...
- ▶ Other topics:
 - ▶ Early stopping of CG as a means of regularization
 - ▶ Hidden cost function modifications like corner rounding
 - ▶ Using NRMSE and SSIM instead of task-relevant metrics
 - ▶ Inverse crimes [6, 38]
- ▶ Take-away
 - ▶ Mathematical foundations can also help develop ML-based IR methods with theoretical underpinnings
 - ▶ **May we live in interesting times...**



- Online demos:
<https://github.com/JeffFessler/book-la-demo>
- Topics include: low-rank matrix approximation, robust PCA, photometric stereo, video foreground/background separation, spectral clustering, matrix completion, ...
- Cambridge Univ. Press, 2024

Talk and code available online at
<http://web.eecs.umich.edu/~fessler>



- [1] Anonymous. "FAST-DIPS: Adjoint-free analytic steps and hard-constrained likelihood correction for diffusion-prior inverse problems." In: *Proc. Intl. Conf. on Learning Representations*. 2026.
- [2] K. P. Pruessmann, M. Weiger, P. Boernert, and P. Boesiger. "Advances in sensitivity encoding with arbitrary k-space trajectories." In: *Mag. Res. Med.* 46.4 (Oct. 2001), 638–51.
- [3] C. A. Baron, N. Dwork, J. M. Pauly, and D. G. Nishimura. "Rapid compressed sensing reconstruction of 3D non-Cartesian MRI." In: *Mag. Res. Med.* 79.5 (May 2018), 2685–92.
- [4] R. E. Gabr, P. Aksit, P. A. Bottomley, A-B. M. Youssef, and Y. M. Kadah. "Deconvolution-interpolation gridding (DING): Accurate reconstruction for arbitrary k-space trajectories." In: *Mag. Res. Med.* 56.6 (Dec. 2006), 1182–91.
- [5] F. Ong, M. Uecker, and M. Lustig. "Accelerating non-Cartesian MRI reconstruction convergence using k-space preconditioning." In: *IEEE Trans. Med. Imag.* 39.5 (2020), 1646–54.
- [6] J. Kaipio and E. Somersalo. "Statistical inverse problems: Discretization, model reduction and inverse crimes." In: *J. Comp. Appl. Math.* 198.2 (Jan. 2007), 493–504.
- [7] M. Guerquin-Kern, D. V. D. Ville, K. Pruessmann, and M. Unser. "Analytical form of Shepp-Logan phantom for parallel MRI." In: *Proc. IEEE Intl. Symp. Biomed. Imag.* 2010, 261–4.
- [8] T. Hong, X. Xu, J. Hu, and J. A. Fessler. "Provable preconditioned plug-and-play approach for compressed sensing MRI reconstruction." In: *IEEE Trans. Computational Imaging* 10 (2024), 1476–88.
- [9] T. Hong, Z. Xu, J. Hu, and J. A. Fessler. "Using randomized Nyström preconditioners to accelerate variational image reconstruction." In: *IEEE Trans. Computational Imaging* 11 (2025), 1630–43.
- [10] M. Blumenthal, T. Holliber, J. I. Tamir, and M. Uecker. *Fast and robust diffusion posterior sampling for MR image reconstruction using the preconditioned unadjusted Langevin algorithm*. 2025.
- [11] D. L. Collins, A. P. Zijdenbos, V. Kollokian, J. G. Sled, N. J. Kabani, C. J. Holmes, and A. C. Evans. "Design and construction of a realistic digital brain phantom." In: *IEEE Trans. Med. Imag.* 17.3 (June 1998), 463–8.

- [12] R. A. Lobos, T. H. Kim, W. S. Hoge, and J. P. Haldar. "Navigator-free EPI ghost correction with structured low-rank matrix models: new theory and methods." In: *IEEE Trans. Med. Imag.* 37.11 (Nov. 2018), 2390–402.
- [13] S. Geman and D. E. McClure. "Bayesian image analysis: an application to single photon emission tomography." In: *Proc. of Stat. Comp. Sect. of Amer. Stat. Assoc.* 1985, 12–8.
- [14] G. Gindi, A. Rangarajan, M. Lee, P. J. Hong, and I. G. Zubal. "Bayesian reconstruction for emission tomography via deterministic annealing." In: *Information Processing in Medical Im.* Ed. by H H Barrett and A F Gmitro. Vol. 687. *Lecture Notes in Computer Science.* Berlin: Springer Verlag, 1993, pp. 322–38.
- [15] A. Goujon, S. Neumayer, and M. Unser. "Learning weakly convex regularizers for convergent image-reconstruction algorithms." In: *SIAM J. Imaging Sci.* 17.1 (2024), 91–115.
- [16] J. R. Chand and M. Jacob. "Convex implicit multi-scale (i-MuSE) energy framework: bridging compressed sensing and diffusion models." In: *Proc. Intl. Soc. Mag. Res. Med.* 2025, p. 5153.
- [17] A. Beck and M. Teboulle. "Fast gradient-based algorithms for constrained total variation image denoising and deblurring problems." In: *IEEE Trans. Im. Proc.* 18.11 (Nov. 2009), 2419–34.
- [18] L. Calatroni and A. Chambolle. "Backtracking strategies for accelerated descent methods with smooth composite objectives." In: *SIAM J. Optim.* 29.3 (Jan. 2019), 1772–98.
- [19] I. Daubechies, M. Defrise, and C. De Mol. "An iterative thresholding algorithm for linear inverse problems with a sparsity constraint." In: *Comm. Pure Appl. Math.* 57.11 (Nov. 2004), 1413–57.
- [20] A. Beck and M. Teboulle. "A fast iterative shrinkage-thresholding algorithm for linear inverse problems." In: *SIAM J. Imaging Sci.* 2.1 (2009), 183–202.
- [21] U. Jang, S. D. Gupta, and E. K. Ryu. *Computer-assisted design of accelerated composite optimization methods: optISTA.* 2023.

- [22] A. B. Taylor, J. M. Hendrickx, and Francois Glineur. "Exact worst-case performance of first-order methods for composite convex optimization." In: *SIAM J. Optim.* 27.3 (Jan. 2017), 1283–313.
- [23] D. Kim and J. A. Fessler. "Adaptive restart of the optimized gradient method for convex optimization." In: *J. Optim. Theory Appl.* 178.1 (July 2018), 240–63.
- [24] C. Y. Lin and J. A. Fessler. "Efficient dynamic parallel MRI reconstruction for the low-rank plus sparse model." In: *IEEE Trans. Computational Imaging* 5.1 (Mar. 2019), 17–26.
- [25] J. A. Fessler. "Optimization methods for MR image reconstruction." In: *IEEE Sig. Proc. Mag.* 37.1 (Jan. 2020), 33–40.
- [26] U. S. Kamilov, C. A. Bouman, G. T. Buzzard, and B. Wohlberg. "Plug-and-play methods for integrating physical and learned models in computational imaging: theory, algorithms, and applications." In: *IEEE Sig. Proc. Mag.* 40.1 (2023), 85–97.
- [27] S. H. Chan, X. Wang, and O. A. Elgendy. "Plug-and-play ADMM for image restoration: fixed-point convergence and applications." In: *IEEE Trans. Computational Imaging* 3.1 (Mar. 2017), 84–98.
- [28] Y. Sun, B. Wohlberg, and U. S. Kamilov. "An online plug-and-play algorithm for regularized image reconstruction." In: *IEEE Trans. Computational Imaging* 5.3 (Sept. 2019), 395–408.
- [29] E. K. Ryu, J. Liu, S. Wang, X. Chen, Z. Wang, and W. Yin. "Plug-and-play methods provably converge with properly trained denoisers." In: *Proc. Intl. Conf. Mach. Learn.* 2019.
- [30] X. Xu, Y. Sun, J. Liu, B. Wohlberg, and U. S. Kamilov. "Provable convergence of plug-and-play priors with MMSE denoisers." In: *IEEE Signal Proc. Letters* 27 (2020), 1280–4.
- [31] P. Nair, R. Gavaskar, and K. Chaudhury. "Fixed-point and objective convergence of plug-and-play algorithms." In: *IEEE Trans. Computational Imaging* 7 (2021), 337–48.
- [32] Y. Sun, Z. Wu, X. Xu, B. Wohlberg, and U. S. Kamilov. "Scalable plug-and-play ADMM With convergence guarantees." In: *IEEE Trans. Computational Imaging* 7 (2021), 849–63.

- [33] H. Y. Tan, S. Mukherjee, J. Tang, and C-B. Schonlieb. “Provably convergent plug-and-play quasi-Newton methods.” In: *SIAM J. Imaging Sci.* 17.2 (2024), 785–819.
- [34] S. Hurault, A. Chambolle, A. Leclaire, and N. Papadakis. “Convergent plug-and-play with proximal denoiser and unconstrained regularization parameter.” In: *J. Math. Im. Vision* 66.4 (June 2024), 616–38.
- [35] T. Hong, Z. Xu, S. Y. Chun, L. Hernandez-Garcia, and J. A. Fessler. “Convergent complex quasi-Newton proximal method for gradient-driven denoisers in compressed sensing MRI reconstruction.” In: *IEEE Trans. Computational Imaging* 11 (2025), 1534–47.
- [36] R. A. Lobos, J-S. Cavazos, R. R. Nadakuditi, and J. A. Fessler. “Smooth optimization using global and local low-rank regularizers.” In: *SIAM J. Imaging Sci.* (2026). To appear.
- [37] R. A. Lobos, J. S. Cavazos, R. R. Nadakuditi, and J. A. Fessler. *Smooth optimization algorithms for global and locally low-rank regularizers*. 2025.
- [38] E. Shimron, J. I. Tamir, K. Wang, and M. Lustig. “Implicit data crimes: Machine learning bias arising from misuse of public data.” In: *Proc. Natl. Acad. Sci.* 119.13 (Mar. 2022), e2117203119.